Electronic Supplementary Material (ESI) for RSC Advances.

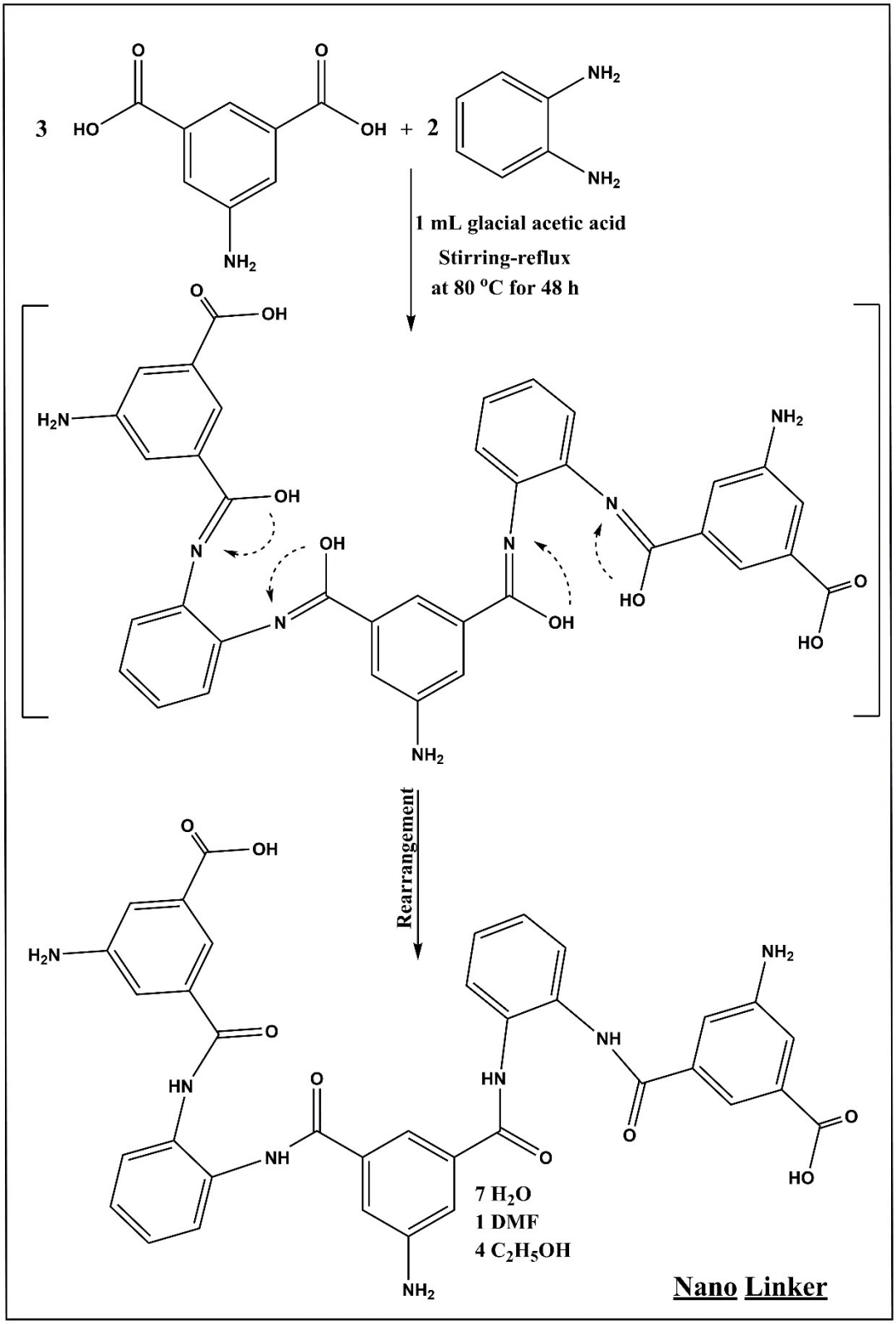

Scheme S1: The proposed mechanism of the nano linker (NL) synthesis.

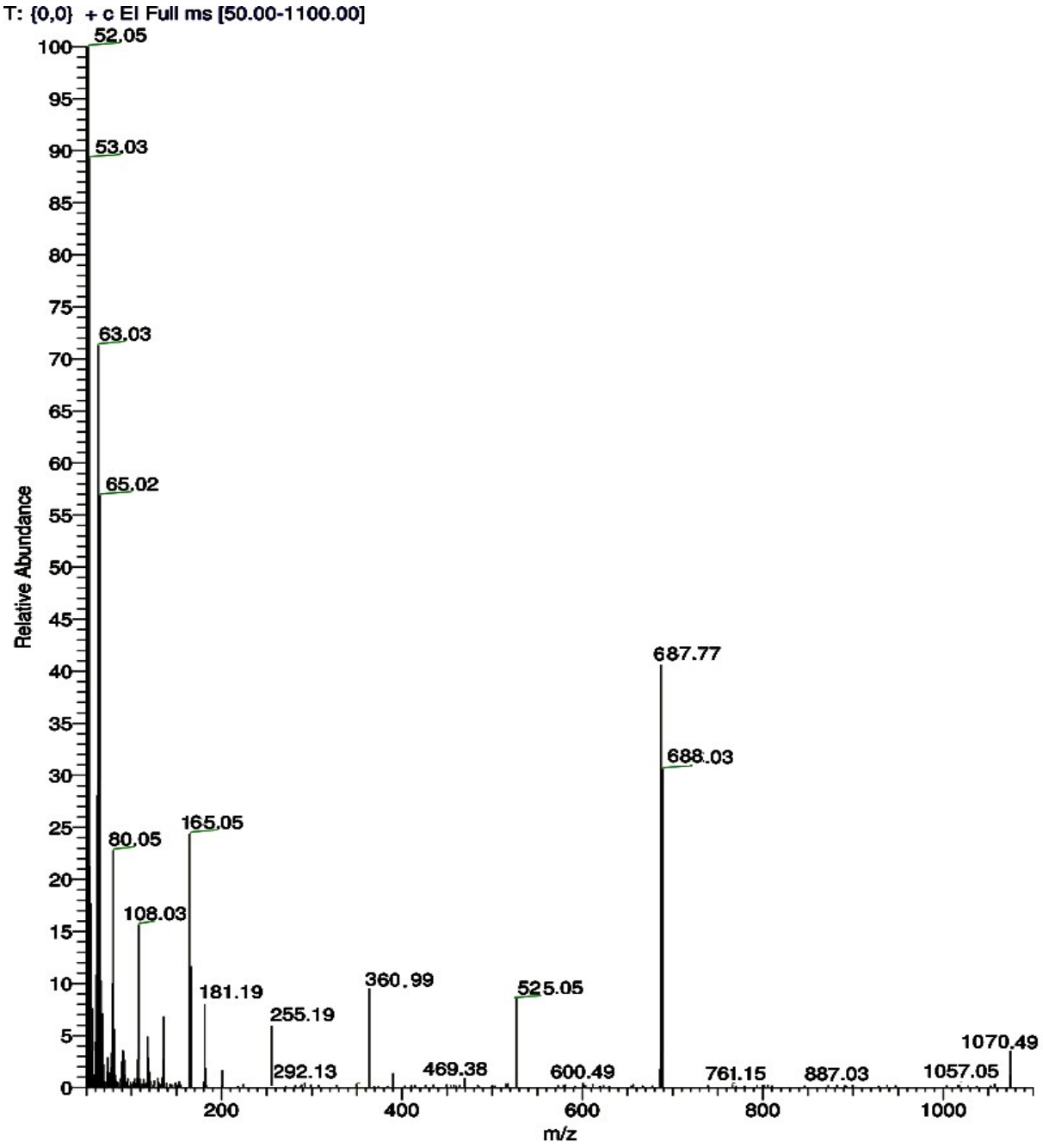

Fig. S2: The mass spectrum of the nano linker (NL)

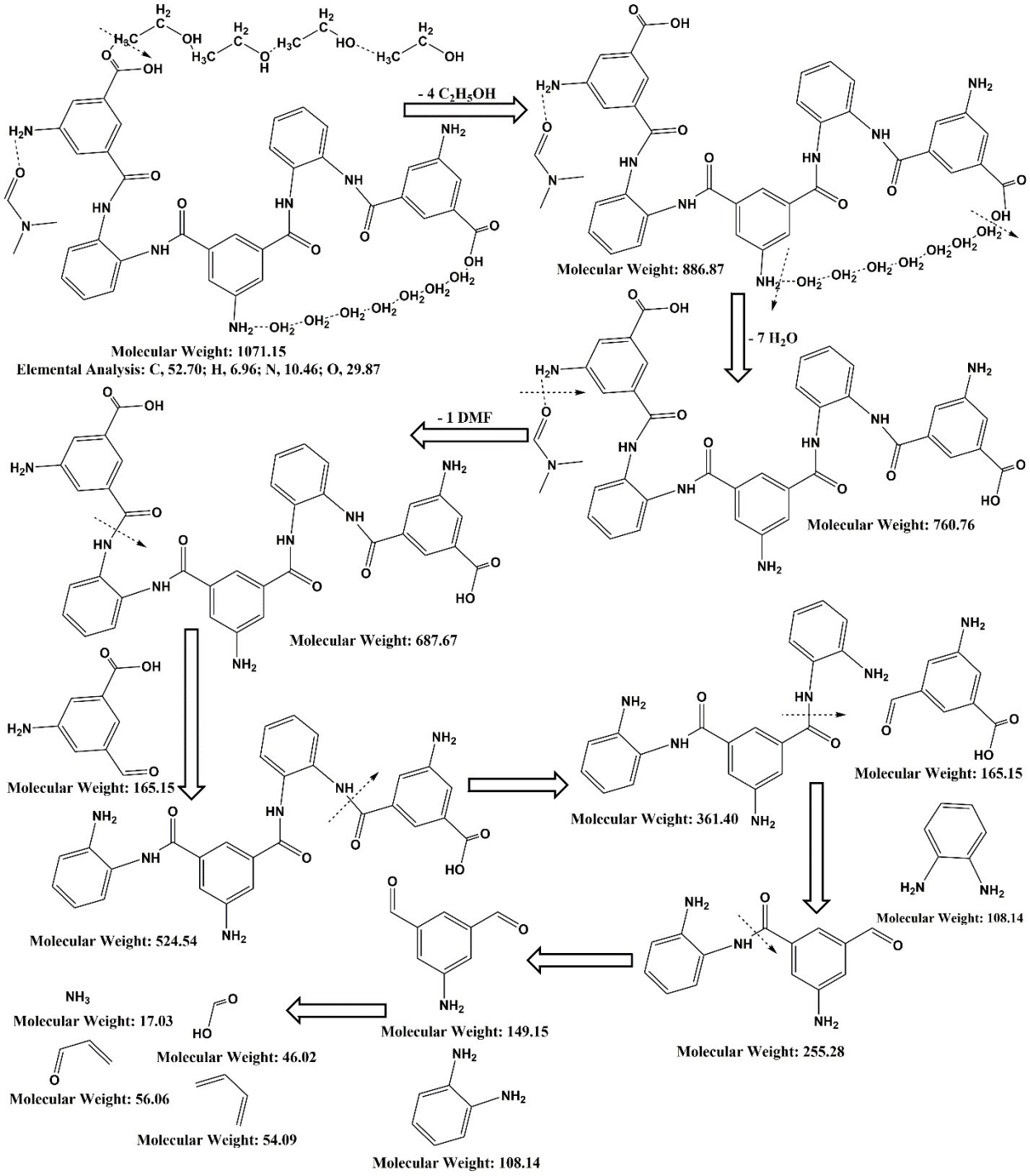

Fig. S3: The proposed fragmentation scheme of the nano linker (NL).

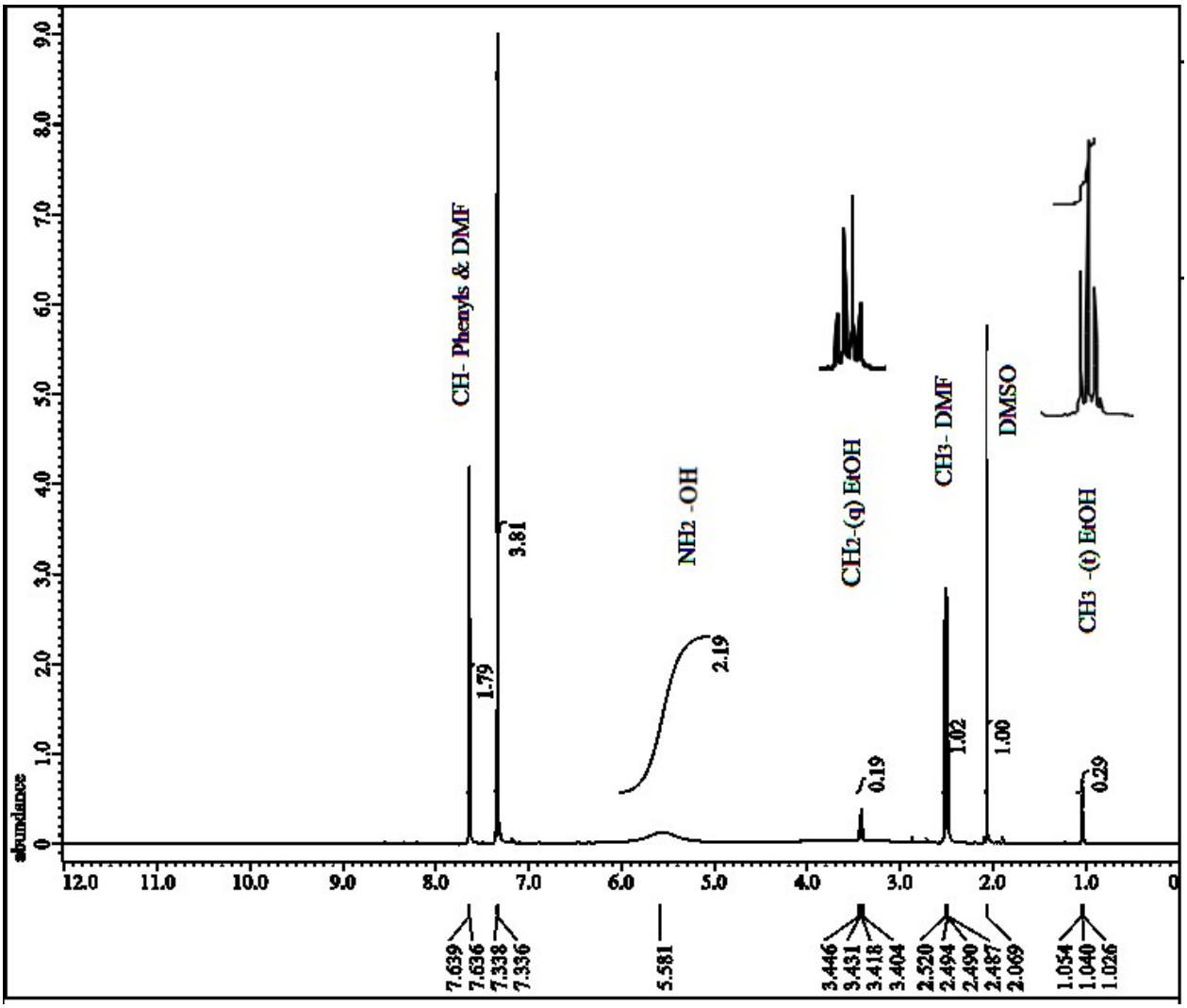

Fig. S4: The ^{1}H-NMR spectrum of nano linker (NL).

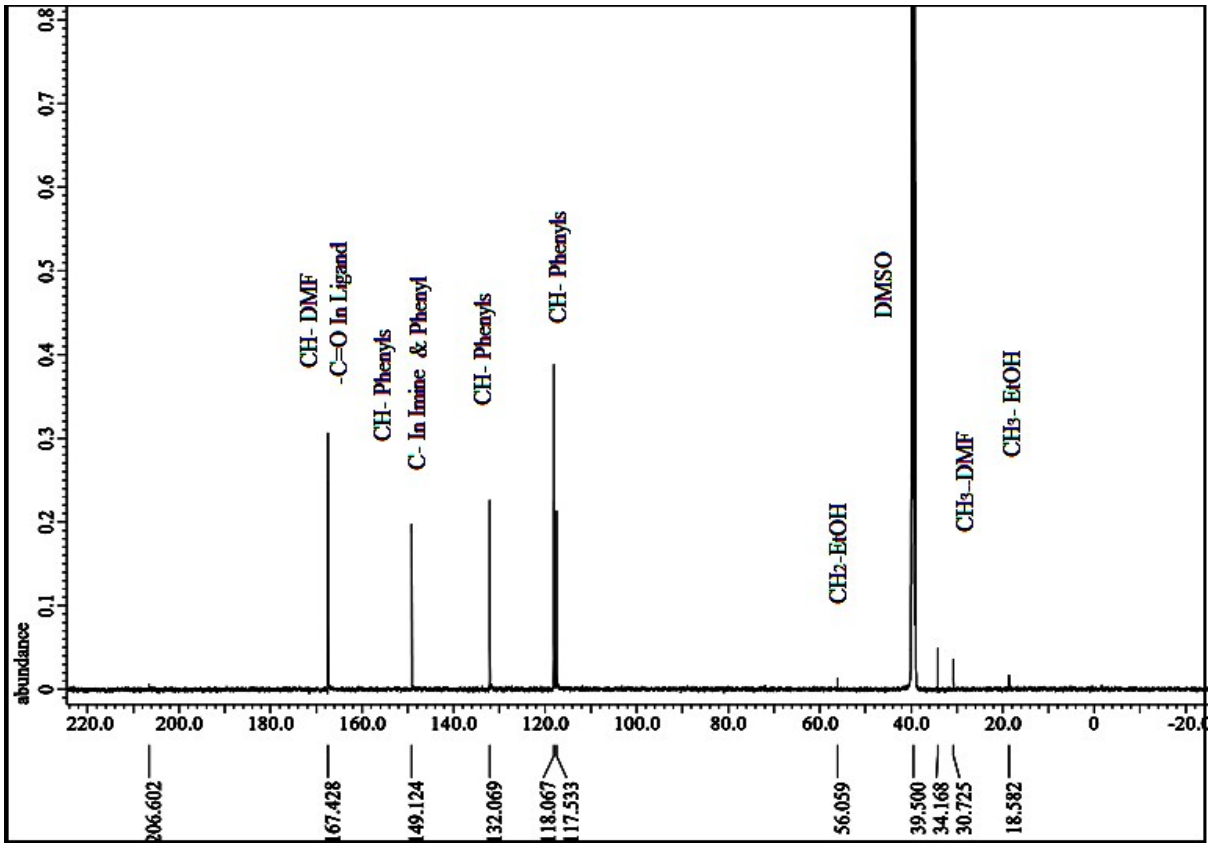

Fig. S5: The ^{13}C-NMR spectrum of nano linker (NL).

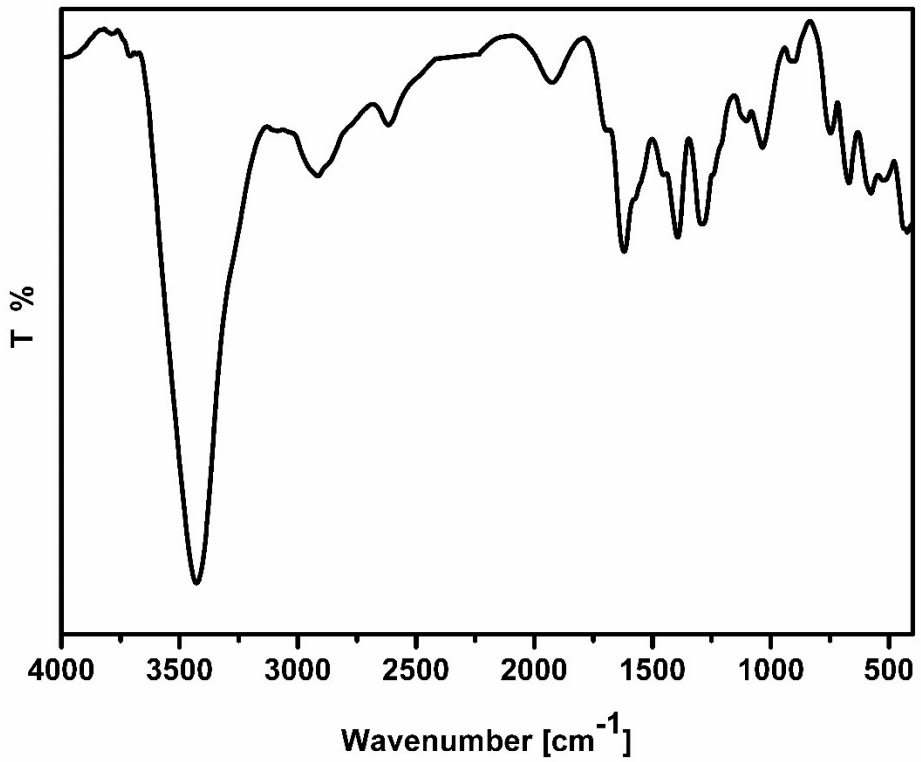

Fig. S6: The FT-IR spectrum of nano linker (NL).

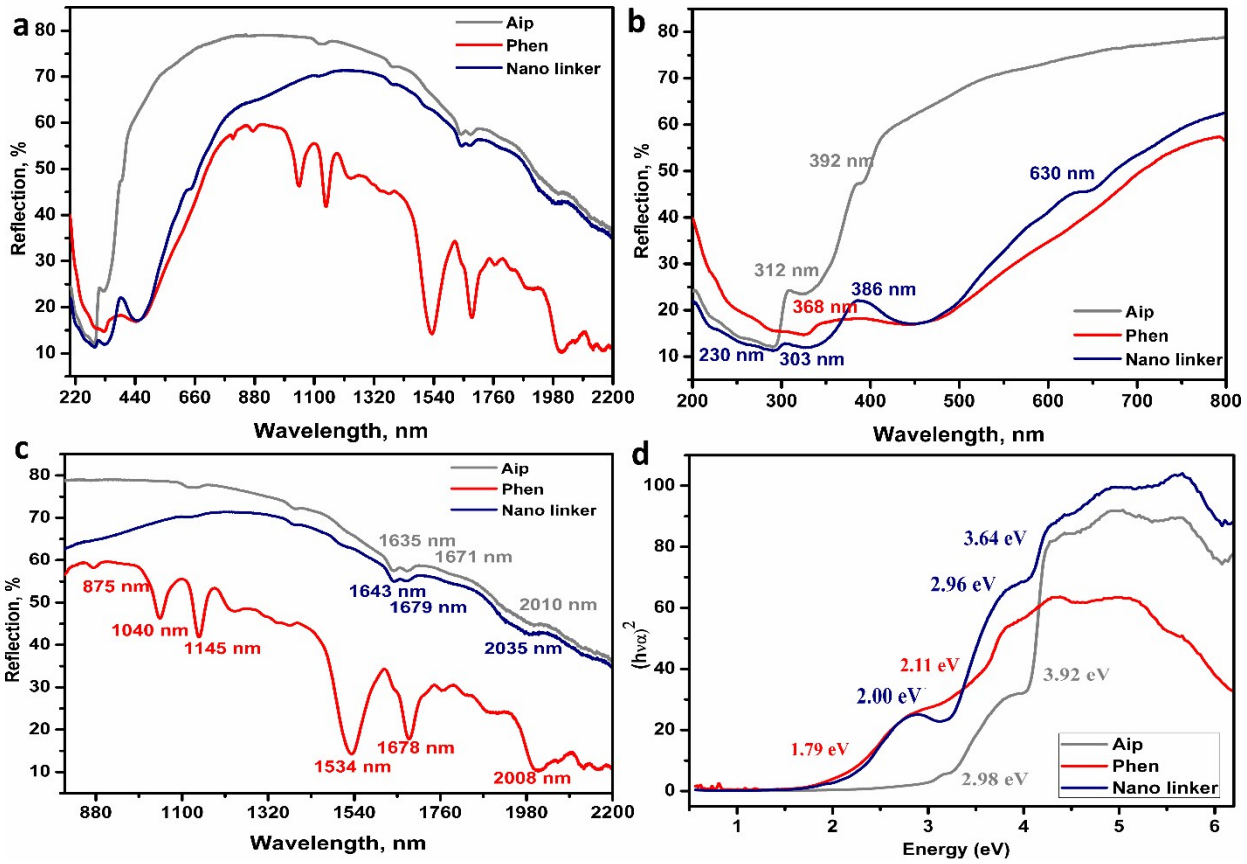

Fig. S7: (a, b, and c) The electronic absorption spectra of Aip, Phen, and NL at different ranges, **(d)** The band gap energy of Aip, Phen, and NL.

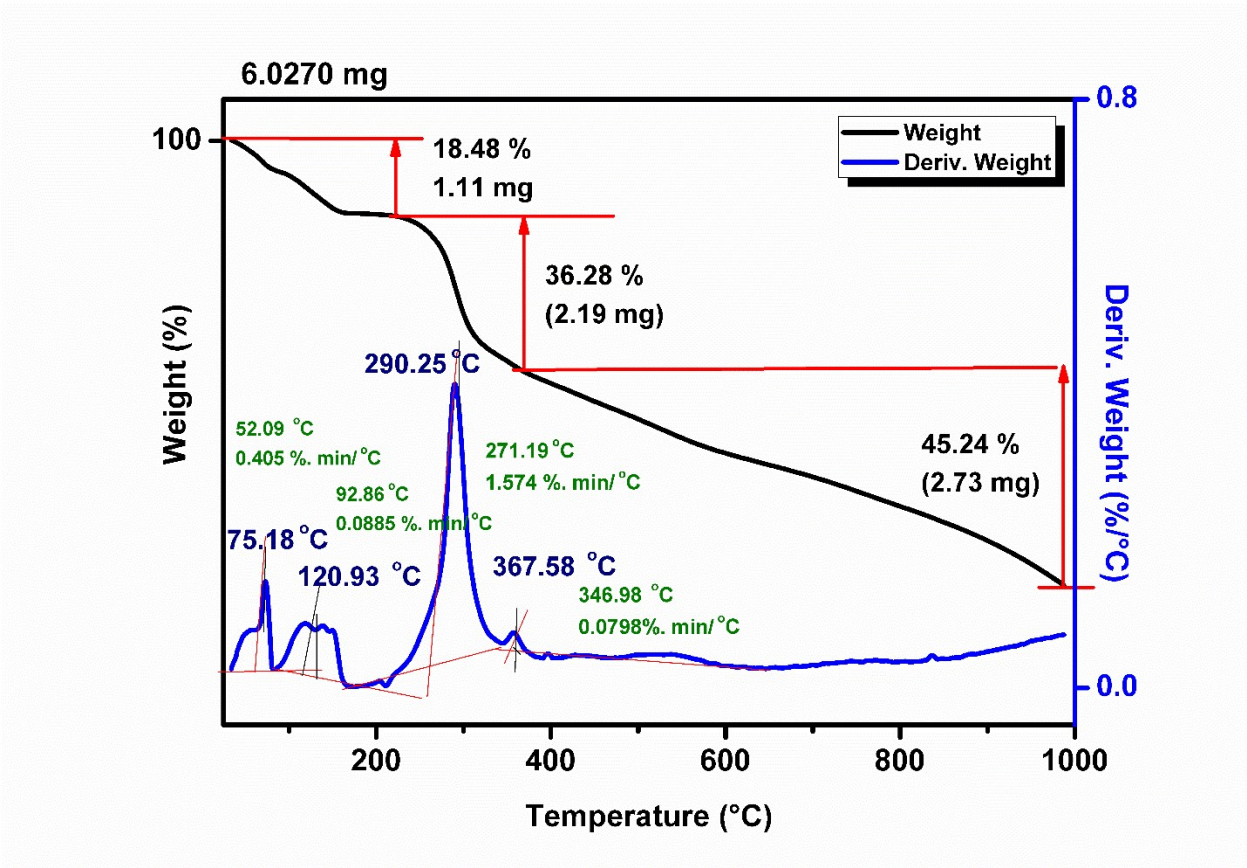

Fig. S8: The thermogravimetric analysis (TGA-DTGA) of the NL.

Table S9: EDX analysis of the NL.

Element	Weight %	Atomic %	Net Int.	Error %
C	52.75	59.25	155.31	6.25
N	10.36	8.05	4.28	16.24
O	36.89	32.7	70.01	11.98

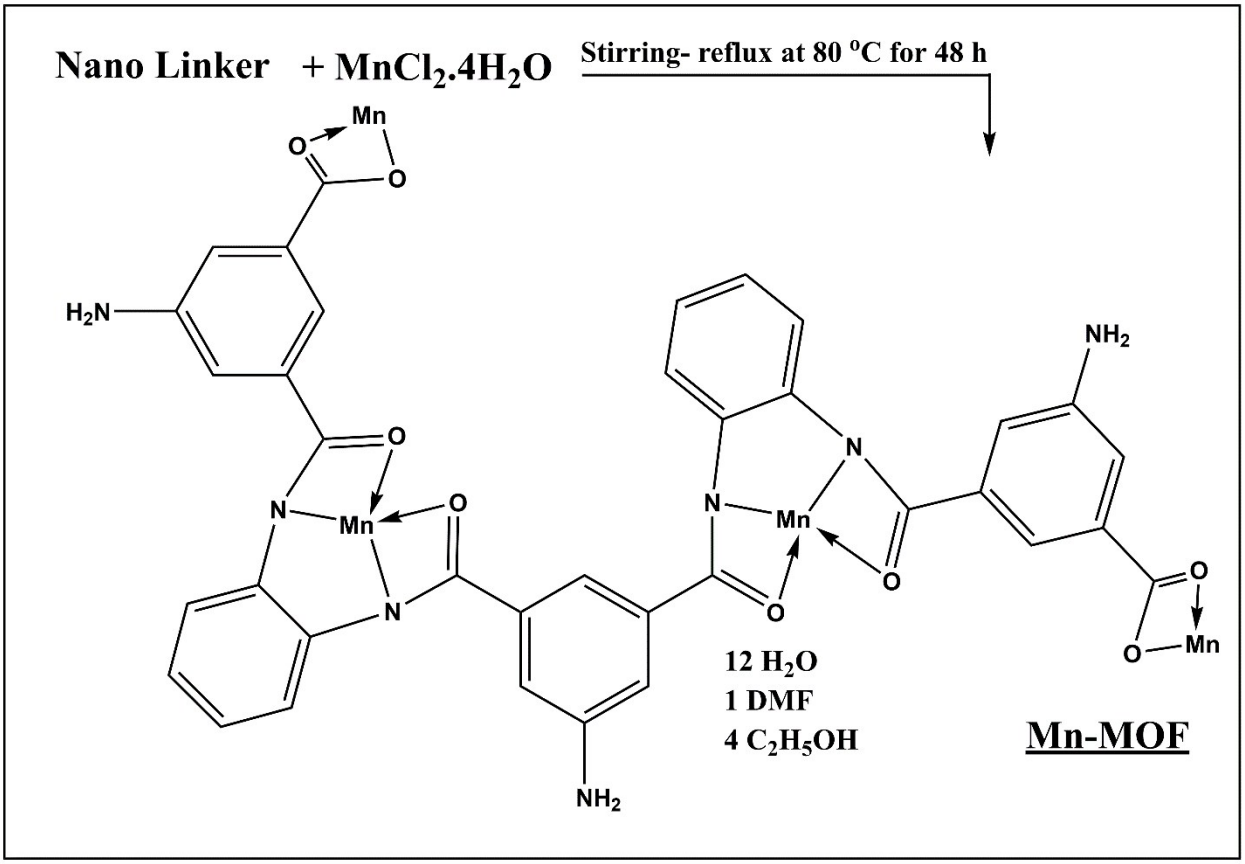

Scheme S10: The proposed mechanism of the Mn-MOF synthesis.

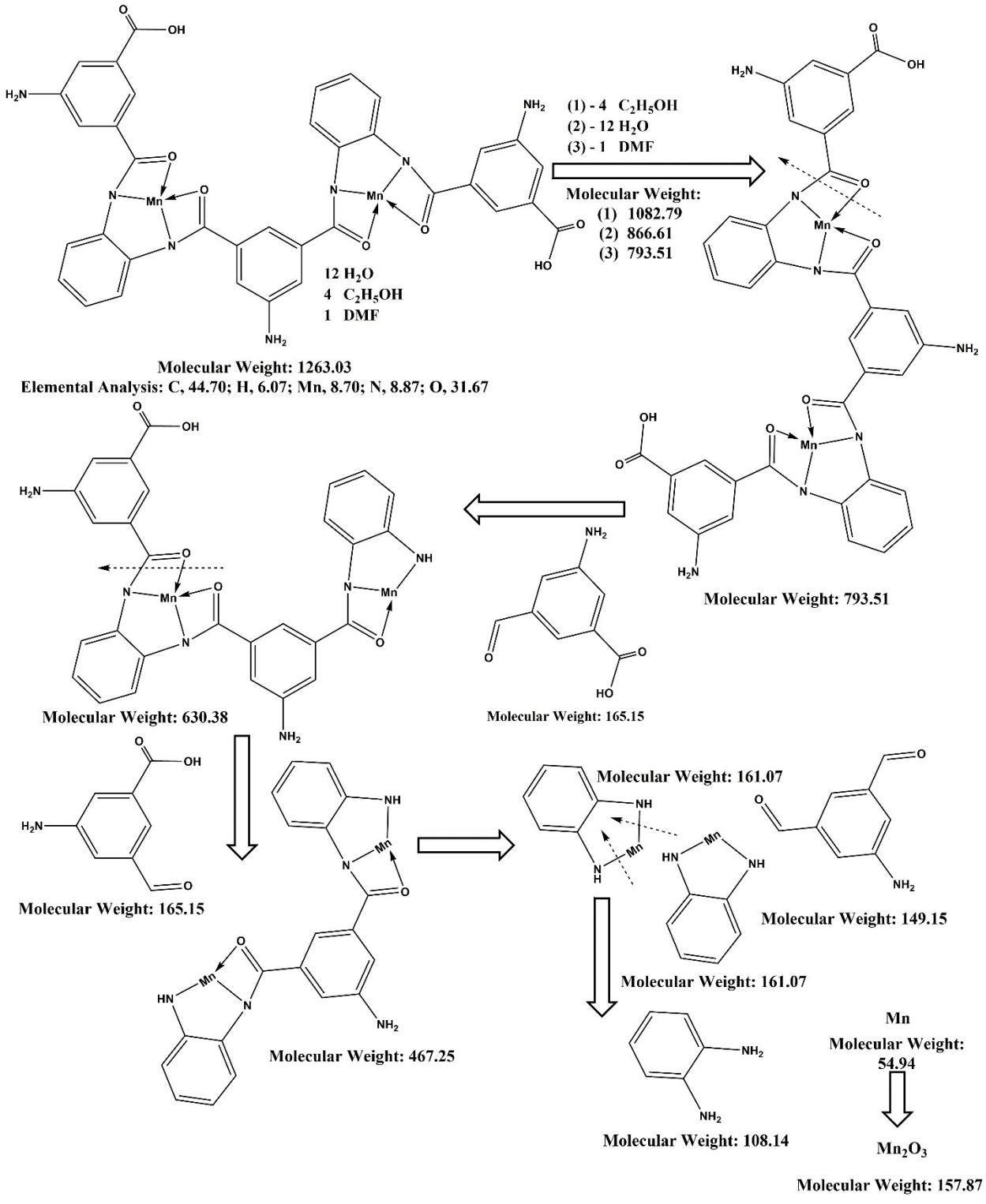

Fig. S11: The proposed fragmentation scheme of the Mn-MOF.

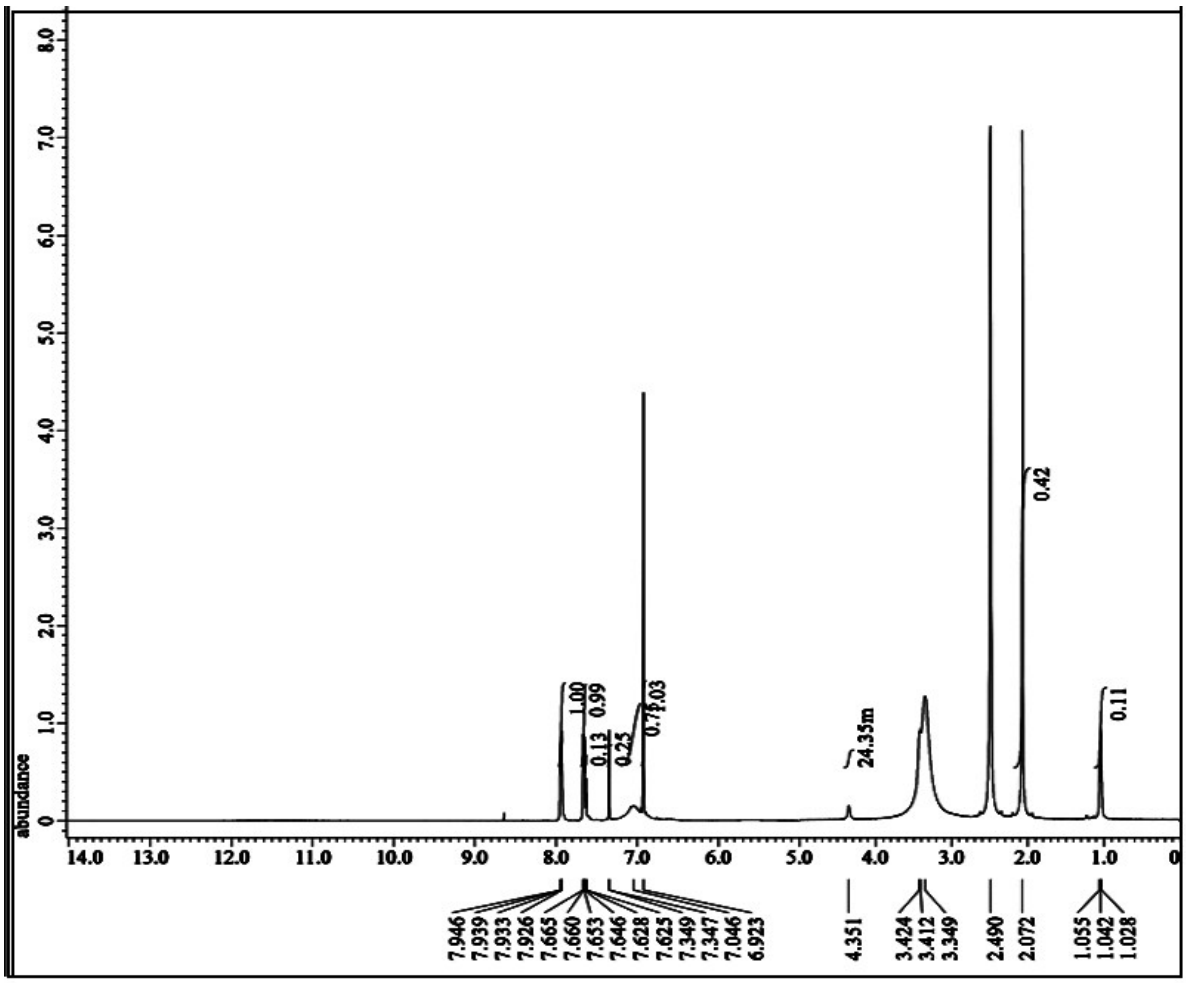

Fig. S12: The ^{1}H-NMR spectrum of the Mn-MOF.

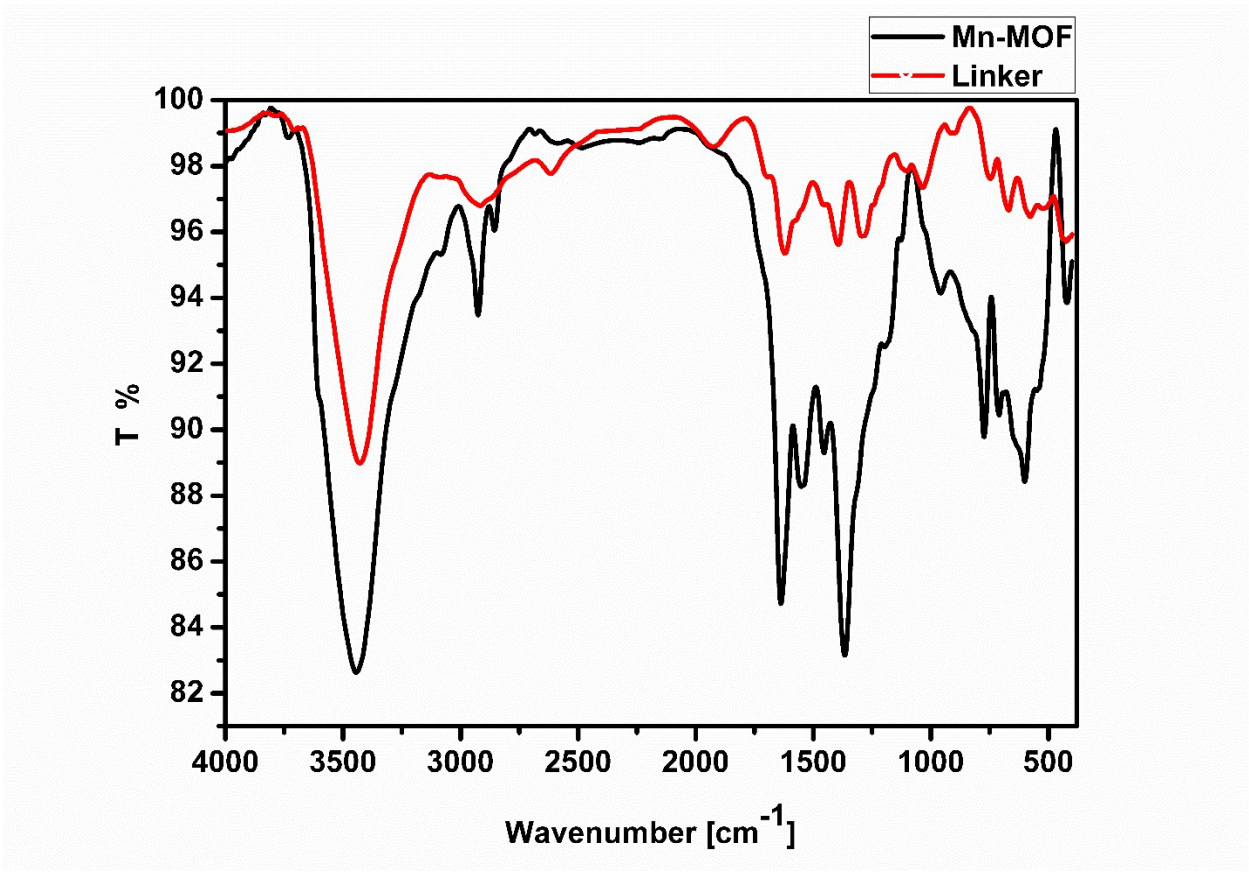

Fig. S13: The FT-IR spectra of the NL and Mn-MOF.

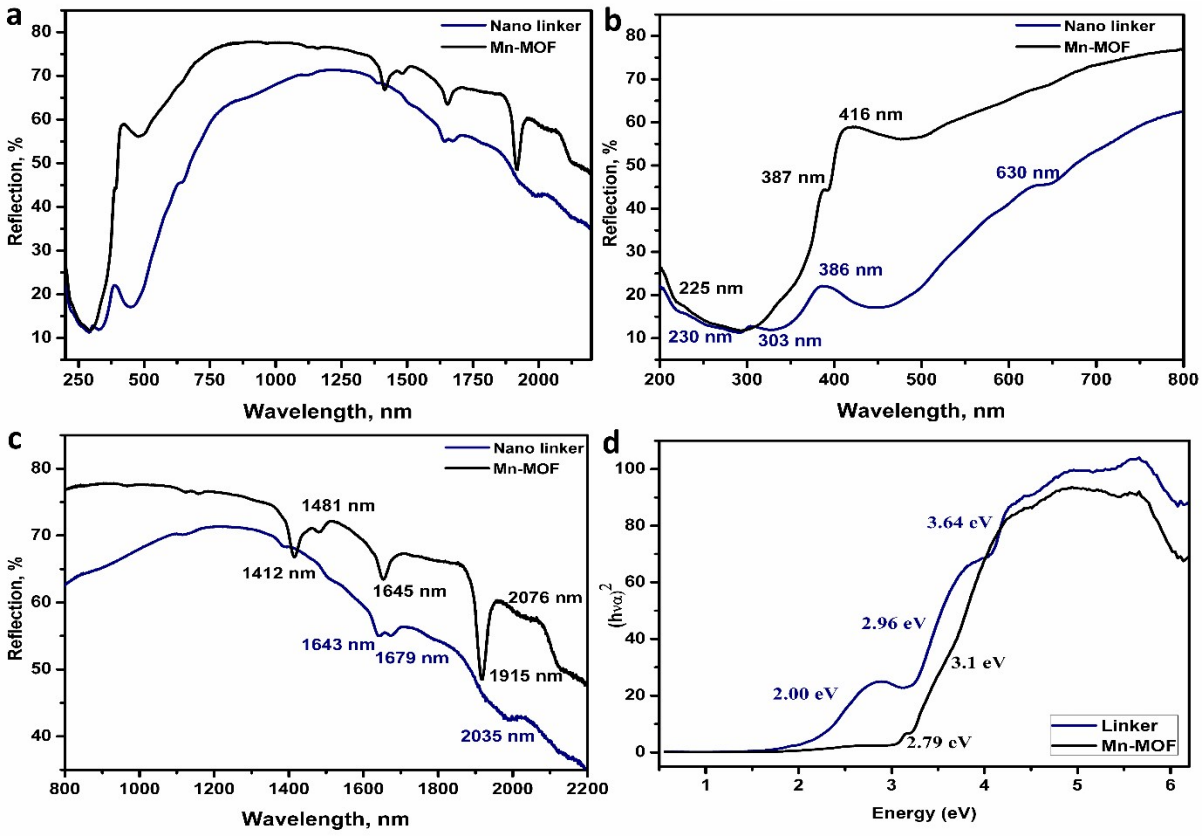

Fig. S14: (a, b, and c) The electronic absorption spectra of the NL and Mn-MOF at different ranges, **(d)** The optical band gap energy of the NL and Mn-MOF.

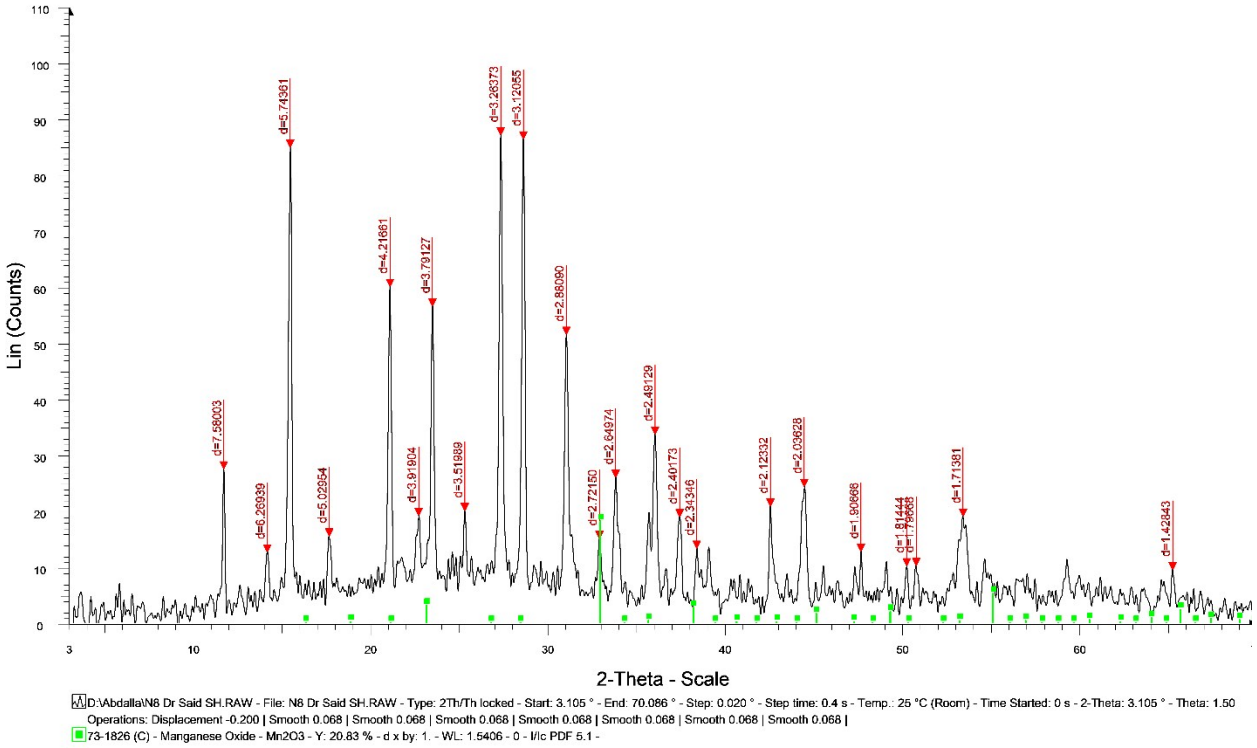

Fig. S15: The X-ray diffraction patterns of the Mn-MOF.

Table S16: Summary of XRD data, Millar indices and interplanar distances of Mn-MOF

Peak No.	2θ	Intensity	Intensity	d value	Θ Radians	Sin θ	Sin 2θ	Ratio 1	Ratio 2	(hkl)
	Å	count	%	Å	Å	Å	Å			
1	11.665	27.5	31.501	7.5802	0.1018	0.1016	0.0103	1	2	
2	14.115	12.7	14.548	6.2695	0.1232	0.1229	0.0151	1.4618	2.9236	
3	15.415	85.2	97.595	5.7435	0.1345	0.1341	0.018	1.1915	2.383	111
4	17.62	15.5	17.755	5.0294	0.1538	0.1532	0.0235	1.3041	2.6083	002
5	21.052	60.2	68.958	4.2166	0.1837	0.1827	0.0334	1.4227	2.8454	021
6	22.671	19.2	21.993	3.919	0.1978	0.1966	0.0386	1.1576	2.3153	
7	23.446	56.7	64.948	3.7912	0.2046	0.2032	0.0413	1.0686	2.1371	121
8	25.282	20.1	23.024	3.5199	0.2206	0.2188	0.0479	1.1601	2.3202	
9	27.303	87.3	100	3.2638	0.2383	0.236	0.0557	1.1631	2.3262	202
10	28.582	86.6	99.198	3.1206	0.2494	0.2468	0.0609	1.0939	2.1878	212
11	31.017	51.6	59.107	2.8809	0.2707	0.2674	0.0715	1.1733	2.3466	
12	32.884	15.1	17.297	2.7215	0.287	0.283	0.0801	1.1206	2.2412	222
13	33.801	26	29.782	2.6497	0.295	0.2907	0.0845	1.0549	2.1098	023
14	36.022	33.8	38.717	2.4913	0.3144	0.3092	0.0956	1.1934	2.3867	213
15	37.414	18.9	21.649	2.4017	0.3265	0.3207	0.1029	1.076	2.1519	
16	38.38	13.3	15.235	2.3435	0.3349	0.3287	0.108	1.0503	2.1007	004
17	42.542	20.8	23.826	2.1233	0.3712	0.3628	0.1316	1.2181	2.4362	133
18	44.455	24.4	27.95	2.0363	0.3879	0.3783	0.1431	1.0873	2.1746	142
19	47.658	12.8	14.662	1.9066	0.4159	0.404	0.1632	1.1406	2.2812	242
20	50.243	10.2	11.684	1.8144	0.4385	0.4245	0.1802	1.1042	2.2084	333
21	50.775	10.2	11.684	1.7967	0.4431	0.4287	0.1838	1.0199	2.0398	342
22	53.419	19.1	21.879	1.7138	0.4662	0.4495	0.202	1.099	2.1981	152
23	65.267	9.47	10.848	1.4284	0.5696	0.5393	0.2908	1.4395	2.879	226

Table S17: Summary of calculated crystallite size of Mn-MOF at different position on XRD patterns

Position	Area	Cry Size L(nm)	Microstrain	RMS Strain(%)
3.602555	0.481147	152.7	0.1	0.1
11.64649	4.562902	96.1	0.1	0.1
14.09831	3.330751	44.3	0.1	0.1
15.39315	22.83284	58.3	0.1	0.1
17.93485	20.21825	3	0.1	0.1
21.02227	14.15183	69.7	0.1	0.1
23.36765	50.80222	3	0.1	0.1
23.43363	8.73104	117	0.1	0.1
27.28584	28.0254	49.3	0.1	0.1
28.55771	23.90066	66.2	0.1	0.1
31.00315	21.24583	32.2	0.1	0.1
32.85082	5.019268	32.4	0.1	0.1
33.80285	9.942127	36.2	0.1	0.1
35.63326	4.023009	68.6	0.1	0.1
35.99059	11.05639	50.6	0.1	0.1
37.36077	5.930203	53.7	0.1	0.1
38.38768	2.829175	64.3	0.1	0.1
39.02342	4.984149	24.2	0.1	0.1
42.55086	5.358178	62.1	0.1	0.1
44.37924	9.889326	42.1	0.1	0.1
50.73838	2.034004	90.9	0.1	0.1
53.34017	14.13539	17	0.1	0.1

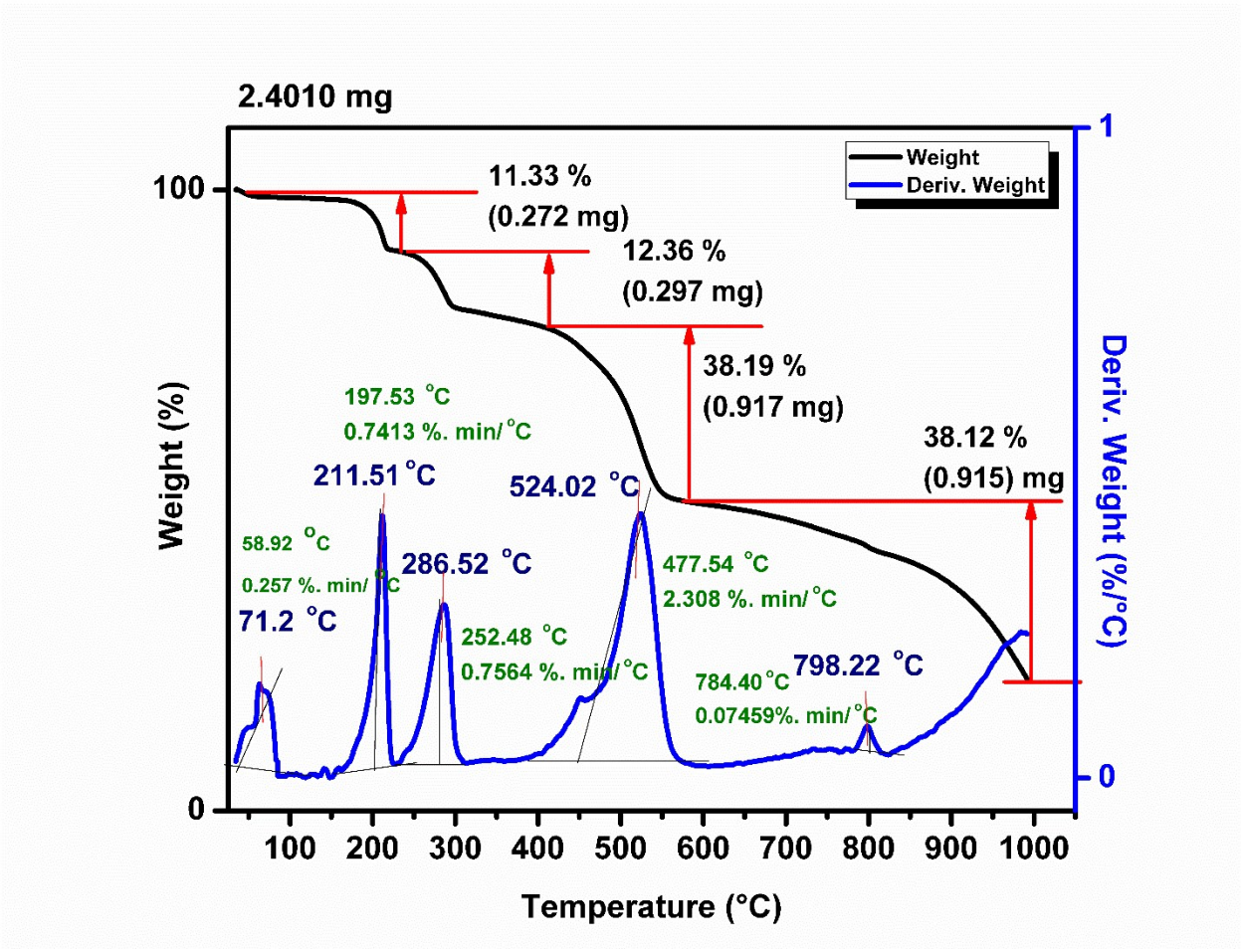

Fig. S18: The thermogravimetric analysis (TGA-DTGA) of the Mn-MOF

Table S19: EDX analysis of the Mn-MOF.

Element	Weight %	Atomic %	Net Int.	Error %
C	44.97	54.09	104.33	7.37
N	8.44	7.98	3.89	29.04
O	37.85	35.88	69.67	11.78
Mn	8.74	2.05	29.13	11.49

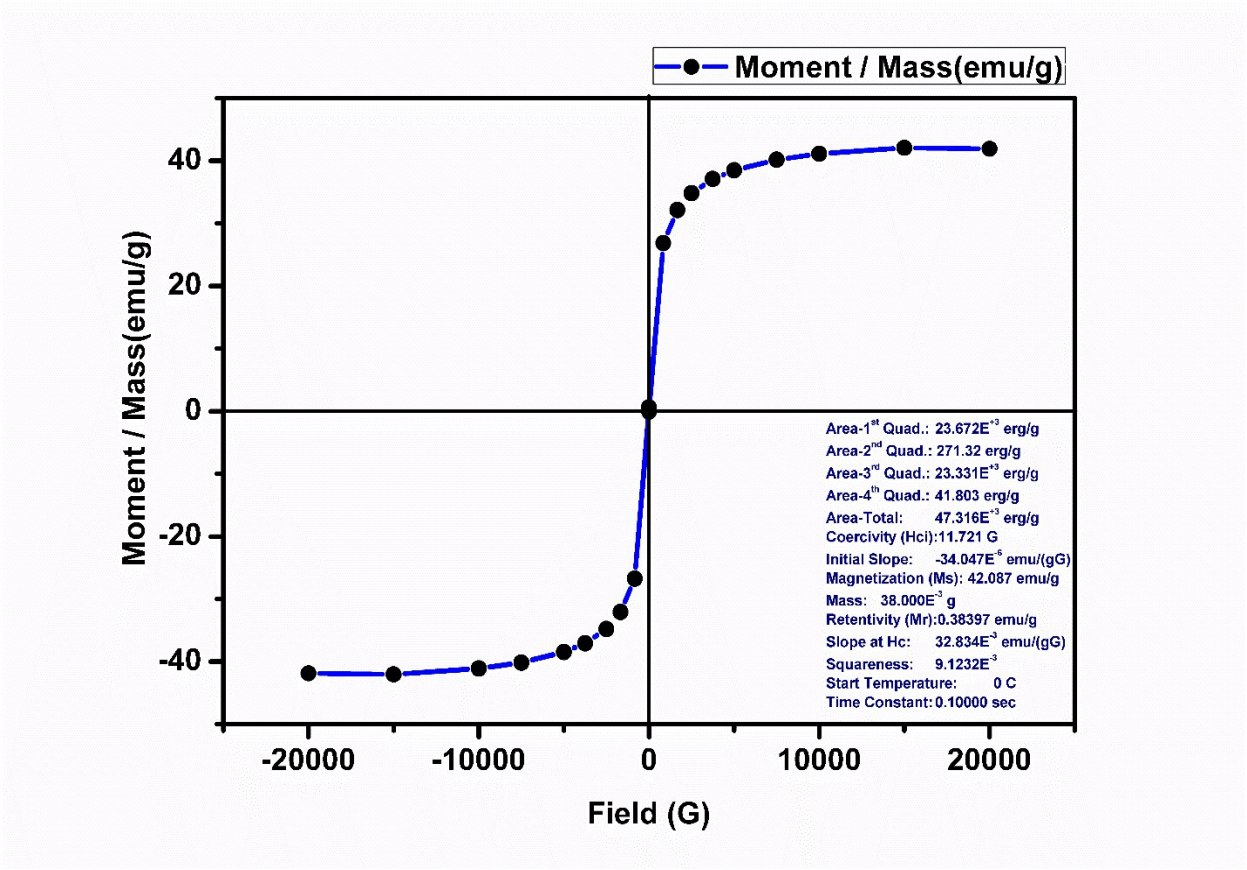

Fig. S20: The magnetization curve of the Mn-MOF.

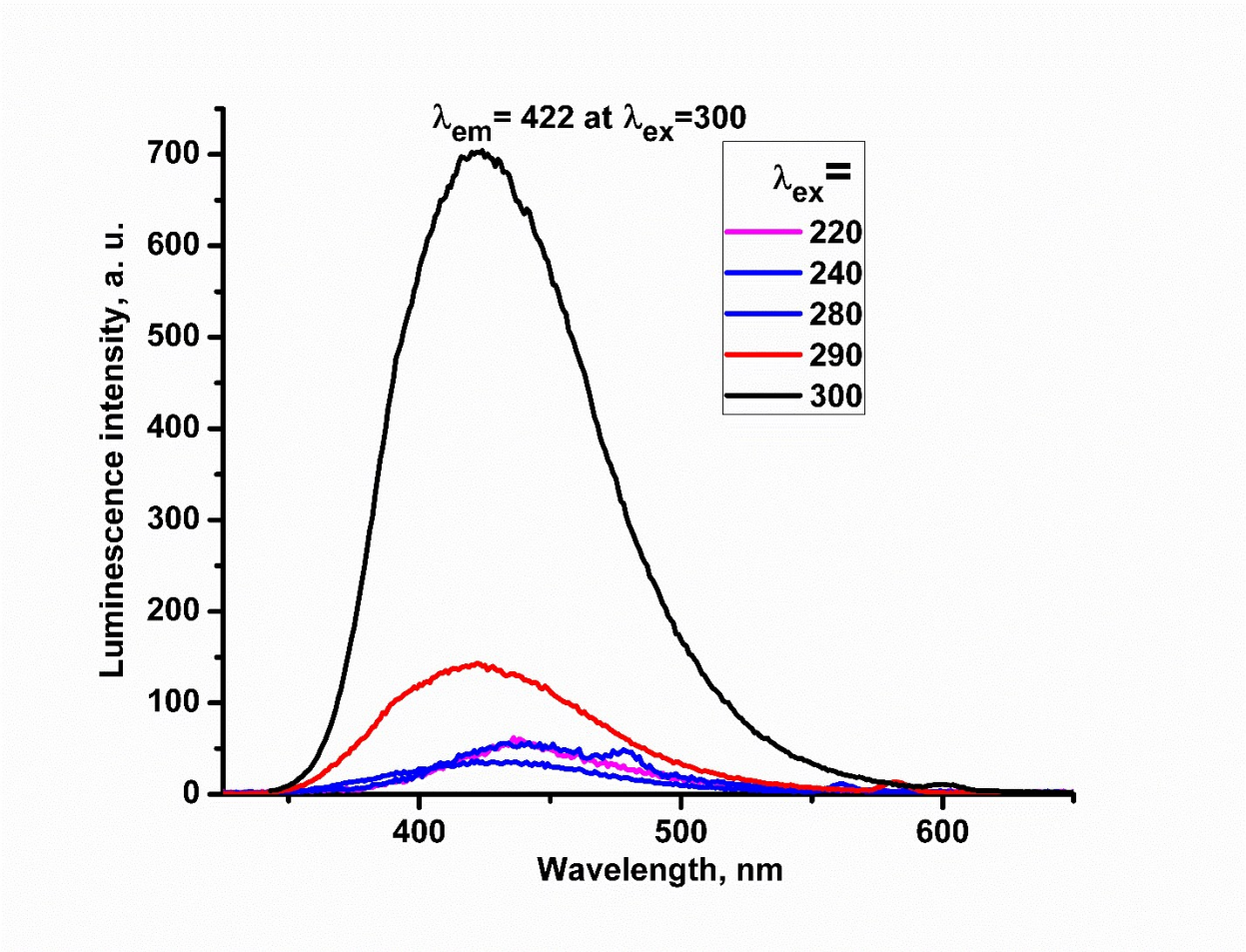

Fig. S21. The PL emission spectra at different excitation wavelength for the Mn-MOF.

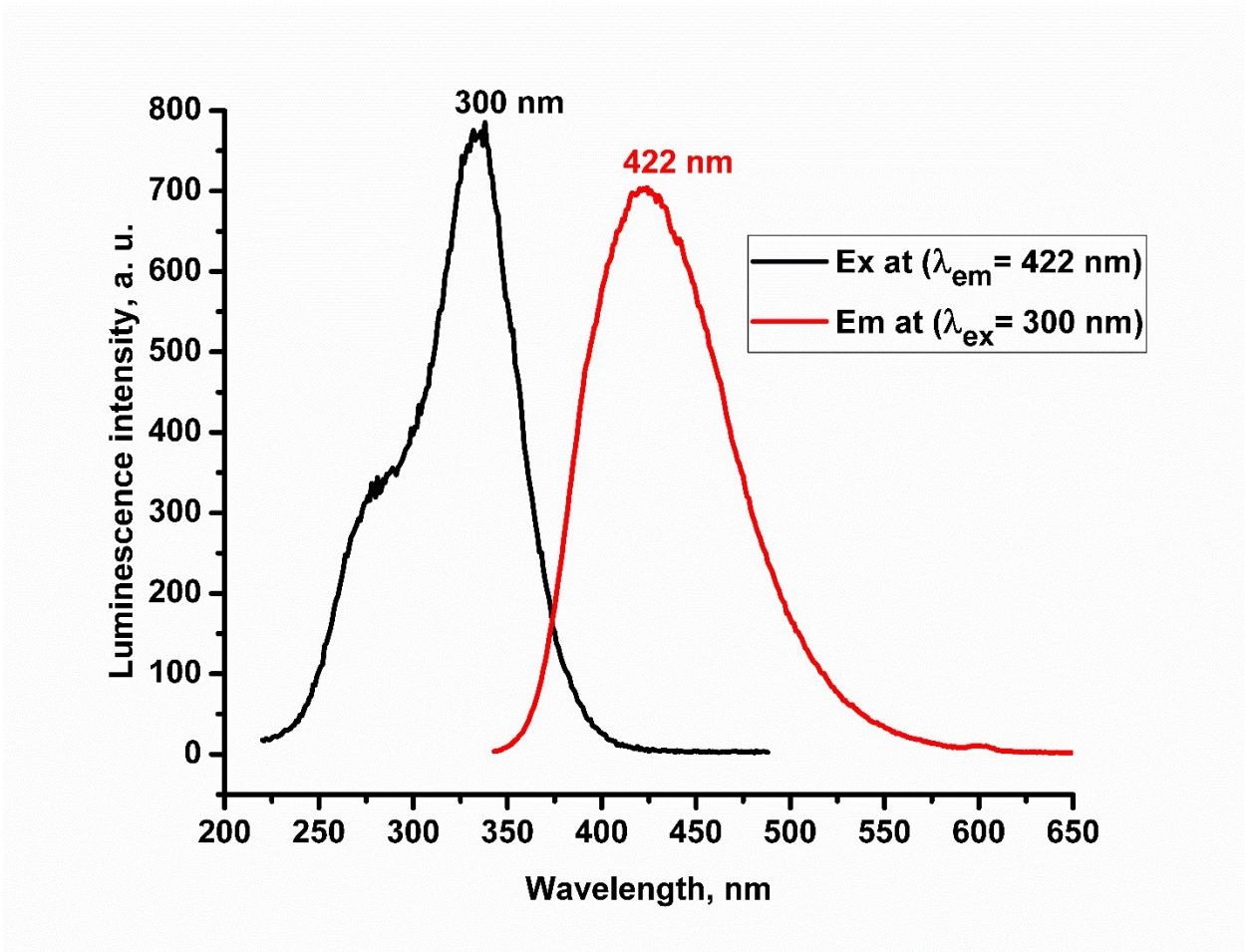

Fig. S22. Excitation (black line) and emission (red line) spectra of Mn-MOF.

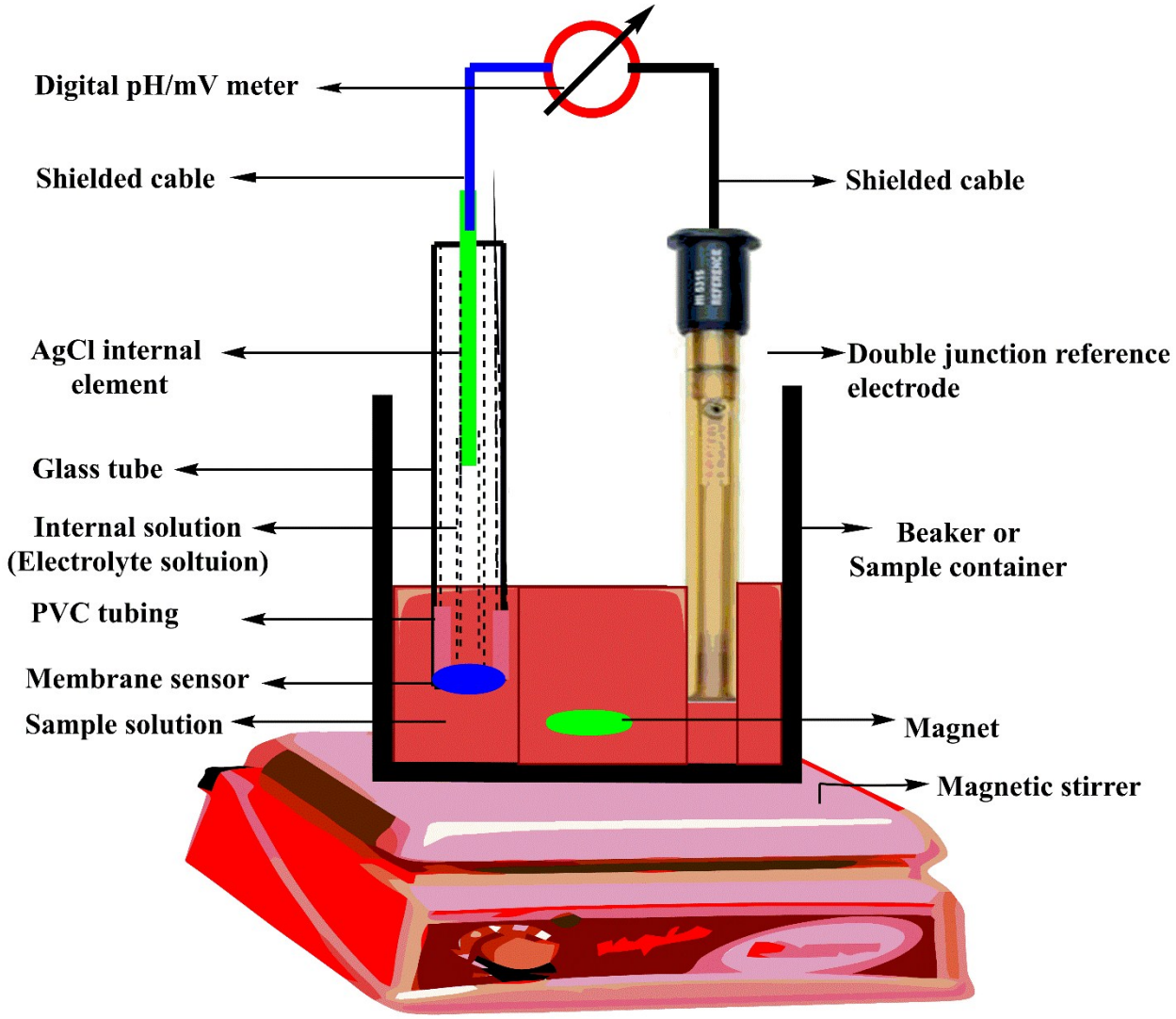

Scheme S23. Schematic diagram of the electrochemical cell for potentiometric measurements.

Table S24: Response characteristics of electrode utilizing various solvent mediators

Solvent mediator	Linear concentration range (ng/mL)	Slope/mV per decade
o-NPOE	0.01 – 30.0	59.0 ± 0.99
DOP	0.25 – 15.0	50.5 ± 1.1
DOS	0.50 – 20.0	48.2 ± 1.2

Table S25: Comparison between the Mn-MOF biosensor and some existing methods for the determination of cTn.

Method	Linear detection range (ng/mL)	LOD (ng/mL)	Reference
Electrochemiluminescent	0.05 – 30.0	0.033	[11]
Ultrasensitive Plasmonic Biosensors	-	0.015	[12]
Ultrasensitive photoelectrochemical immunosensor	0.00002 -50.0	6.7 fg/mL	[13]
Ultrasensitive label-free optical microfibe	2.0 – 10.0 fg/mL	2.0 fg/mL	[14]
Enzyme-linked immunosorbent assay	-	0.1	[34]
Mn-MOF biosensor	0.01 – 30.0	0.055	Present work

Table S26: Selectivity coefficients $K_{A,B}^{pot}$ for various interfering analytes using separate solution method.

Interfering analyte	$K_{A,B}^{pot}$
Cu^{+2}	3.95×10^{-4}
Mn^{+2}	1.39×10^{-4}
Cl^{-}	1.40×10^{-4}
Glucose	1.38×10^{-4}
Lactose	1.36×10^{-4}
Starch	1.36×10^{-4}
Citric acid	1.35×10^{-4}
CK-Total	1.42×10^{-4}
CK-MB	1.42×10^{-4}
PSA	1.43×10^{-4}
CEA	1.41×10^{-4}
Biotin	1.38×10^{-4}
Bilirubin	1.34×10^{-4}
Cholesterol	1.38×10^{-4}
Triglyceride	1.34×10^{-4}
Caffeine	1.35×10^{-4}

Table S27: Evaluation of intra-day, inter-day accuracy, precision, and results of recovery study using spiking technique.

Standard cTn Added, ng/mL*	Repeatability Intra-day precision				Reproducibility Inter-day precision				cTn recovery (Percent ± SD)	
	X	SD	CV	RE%	X	SD	CV	RE%	Intra-day	Inter-day
0.1	0.101	0.004	2E-05	0.993	0.098	0.003	9E-06	0.983	100.7 ±0.004	98.34 ± 0.003
2.0	1.947	0.021	4E-04	1.027	1.955	0.03	9E-04	0.978	97.33 ±0.021	97.75 ± 0.03
20.0	19.6	0.203	0.041	1.02	20.02	0.236	0.056	1.001	98.02 ±0.203	100.1 ± 0.236

* Each reading was repeated Five times; X, mean values; SD, standard deviation; CV, the coefficient of variation; %RE, percent of relative error.

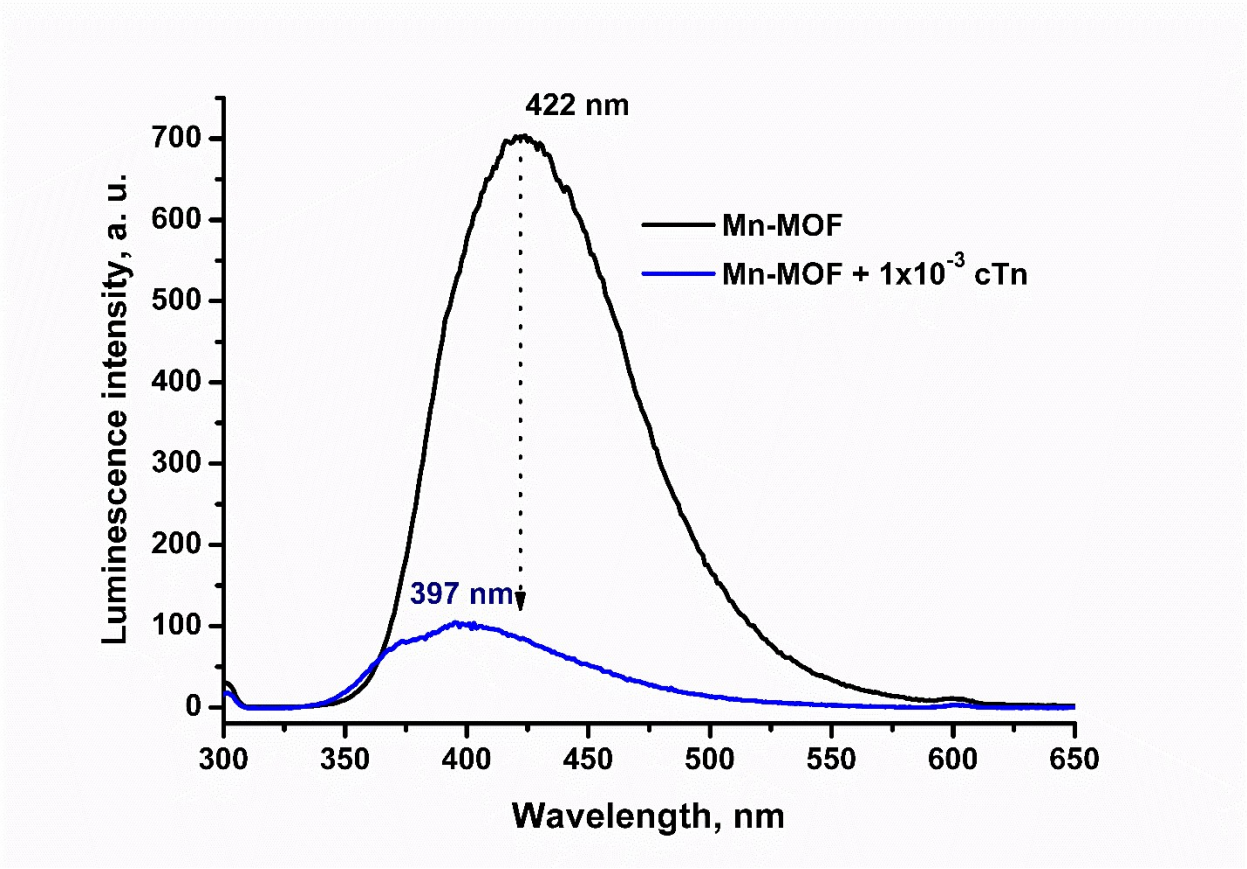

Fig. S28: The PL spectra response for behavior of the Mn-MOF towards cTn.

Appendix A:

References: (1–62)

1. Keller T, Wanner C, Krane V, Kraus D, Genser B, Scharnagl H, et al. Prognostic Value of High-Sensitivity Versus Conventional Cardiac Troponin T Assays Among Patients With Type 2 Diabetes Mellitus Undergoing Maintenance Hemodialysis. American Journal of Kidney Diseases. 2018;71(7):822–830.
2. Shahzad F, Zaidi SA, Koo CM. Highly sensitive electrochemical sensor based on environmentally friendly biomass-derived sulfur-doped graphene for cancer biomarker detection. Sensors and Actuators, B: Chemical [Internet]. 2017;241:716–24. Available from: http://dx.doi.org/10.1016/j.snb.2016.10.144
3. Elliott M. A., Milenko J. T., Bruce T., Mark S., Carolyn H., Christopher P. C., George A. F., Anthony Y. F., Christopher T., Donald W. EB. Cardiac-specific troponin i levels to predict the risk of mortality in patients with acute coronary syndromes. The New England Journal of Medicine. 1996;335(18):1342–9.
4. Thygesen K, Mair J, Katus H, Plebani M, Venge P, Collinson P, et al. Recommendations for the use of cardiac troponin measurement in acute cardiac care †. Eur Heart J. 2010;31(June 2009):2197–206.
5. Alicia A. In New Guideline, A Road Map to Troponin Testing Eating Disorders : Doctors ' Secret Battle Guidance on Troponin Testing. Chest Physician. 2012;7(12):1–2.
6. Giuliani I, Bertinchant J, Granier C, Laprade M, Chocron S, Etievent J, et al. Determination of Cardiac Troponin I Forms in the Blood of Patients with Acute Myocardial Infarction and Patients Receiving Crystalloid or Cold Blood Cardioplegia. Clinical Chemistry. 1999;45(2):213–22.
7. Davies E, Gawad Y, Takahashi M, Shi Q, Lam P, Styba G, et al. Analytical Performance and Clinical Utility of a Sensitive Immunoassay for Determination of Human Cardiac Troponin I. Clinical Biochemistry. 1997;30(6):479–90.
8. Swiderek K, Jaquet K, Meyer HE, Jr LMGH. Cardiac troponin I , isolated from bovine heart , contains two adjacent phosphoserines A first example of phosphoserine determination by derivatization to S-ethylcysteine. Eur J Biochem. 1988;176(2):335–42.
9. Negahdary M., Behjati-Ardakani M. SN, H. H. An Aptamer-based Biosensor for Troponin I Detection in Diagnosis of Myocardial Infarction. J Biomed Phys Eng. 2018;8(2):167–78.
10. Mueller C, Patrono C, Valgimigli M, Collet J, Roffi M. Questions and answers on diagnosis and risk assessment: a companion document of the 2015 ESC Guidelines for the management of acute coronary syndromes in patients presenting without persistent ST-segment elevation. Eur Heart J. 2015;37(3):e15–e21.
11. Palladino P, Minunni M, Scarano S. Cardiac Troponin T capture and detection in real-time via epitope-imprinted polymer and optical biosensing. Biosensors and Bioelectronic [Internet]. 2018;106(2):93–8. Available from: https://doi.org/10.1016/j.bios.2018.01.068
12. Yeon S, Duk Y, Kim K, Sik S, Yoon HC. A fluoro-microbead guiding chip for simple and

quantifiable immunoassay of cardiac troponin I (cTnI). Biosensors and Bioelectronics [Internet]. 2011;26(9):3818–24. Available from: http://dx.doi.org/10.1016/j.bios.2011.02.036

13. Kim K, Park C, Kwon D, Kim D, Meyyappan M, Jeon S, et al. Silicon Nanowire Biosensors for Detection of Cardiac Troponin I (cTnI) with High Sensitivity. Biosensors and Bioelectronic [Internet]. 2015; Available from: http://dx.doi.org/10.1016/j.bios.2015.10.008

14. Missov E, Mair J. A novel biochemical approach to congestive heart failure : Cardiac troponin T. American Heart Journal. 1999;138(1):95–9.

15. Fireman R, Kelly R, Lins V, Tatsuo L. Surface plasmon resonance immunosensor for human cardiac troponin T based on self-assembled monolayer. Journal of Pharmaceutical and Biomedical Analysis. 2007;43:1744–50.

16. Kalra S. High sensitivity troponin. The Bulletin. 2013;8(2):1–6.

17. Tang M, Zhou Z, Shangguan L, Zhao F, Liu S. Electrochemiluminescent detection of cardiac troponin I by using soybean peroxidase labeled-antibody as signal ampli fi er. Talanta [Internet]. 2018;180(December 2017):47–53. Available from: https://doi.org/10.1016/j.talanta.2017.12.015

18. Mayilo S, Kloster MA, Wunderlich M, Lutich A, Klar TA, Nichtl A, et al. Long-Range Fluorescence Quenching by Gold Nanoparticles in a Sandwich Immunoassay for Cardiac Troponin T. Nano Letters. 2009;9(12):4558–63.

19. James SK, Lindahl B, Armstrong P, Califf R, Simoons ML, Venge P, et al. A rapid troponin I assay is not optimal for determination of troponin status and prediction of subsequent cardiac events at suspicion of unstable coronary syndromes. International Journal of Cardiology. 2004;93:113–20.

20. Müller-bardorff M, Sylvén C, Jørgensen B, Collinson PO, Hirschl MM, Anton N, et al. Evaluation of a Point-of-Care System for Quantitative Determination of Troponin T and Myoglobin. Clin Chem Lab Med. 2000;38(6):567–74.

21. Heeschen C, Goldmann BU, Moeller RH, Hamm CW. Analytical performance and clinical application of a new rapid bedside assay for the detection of serum cardiac troponin I. Clinical Chemistry 44:9. 1998;44(9):1925–30.

22. Guo ZR, Gu CR, Fan X, Bian ZP, Wu HF, Yang D, et al. Fabrication of Anti-human Cardiac Troponin I Immunogold Nanorods for Sensing Acute Myocardial Damage. Nanoscale Res Lett. 2009;4:1428–33.

23. Chua JH, Chee R, Agarwal A, Wong SM, Zhang G. Label-Free Electrical Detection of Cardiac Biomarker with Complementary Metal-Oxide Semiconductor-Compatible Silicon Nanowire Sensor Arrays. Analytical Chemistry. 2009;81(15):6266–71.

24. Apple FS, Murakami MM, Christenson RH, Campbell JL, Miller CJ, Hock KG, et al. Analytical performance of the i-STAT cardiac troponin I assay. Clinica Chimica Acta. 2004;345:123–7.

25. Wei J, Mu Y, Song D, Fang X, Liu X, Bu L, et al. A novel sandwich immunosensing method for measuring cardiac troponin I in sera. Analytical Biochemistry. 2003;321:209–16.

26. Lee J, Choi Y, Lee Y, Lee HJ, Lee JN, Kim SK, et al. Sensitive and Simultaneous Detection of Cardiac Markers in Human Serum Using Surface Acoustic Wave Immunosensor. Analytical Chemistry. 2011;83:8629–35.

27. Tsai J, Jung C, Ikoma T, Yoshioka T, Cross JS, Chang S, et al. Surface plasmon resonance biosensor with high anti-fouling ability for the detection of cardiac marker troponin T. Analytica Chimica Acta [Internet]. 2011;703(1):80–6. Available from: http://dx.doi.org/10.1016/j.aca.2011.07.019

28. Mcdonnell B, Hearty S, Leonard P, Kennedy RO. Cardiac biomarkers and the case for point-of-care testing. Clinical Biochemistry [Internet]. 2009;42(7–8):549–61. Available from: http://dx.doi.org/10.1016/j.clinbiochem.2009.01.019

29. Lee I, Luo X, Huang J, Cui XT, Yun M. Detection of Cardiac Biomarkers Using Single Polyaniline Nanowire-Based Conductometric Biosensors. Biosensors. 2012;2:205–20.

30. Qureshi A, Gurbuz Y, Niazi JH. Biosensors for cardiac biomarkers detection : A review. Sensors & Actuators: B Chemical [Internet]. 2012;171–172:62–76. Available from: http://dx.doi.org/10.1016/j.snb.2012.05.077

31. Zhang G, Tshun K, Chai C, Zhan H, Luo H, Min J, et al. Multiplexed detection of cardiac biomarkers in serum with nanowire arrays using readout ASIC. Biosensors and Bioelectronics [Internet]. 2012;35(1):218–23. Available from: http://dx.doi.org/10.1016/j.bios.2012.02.052

32. Lotze U, Lemm H, Heyer A, Müller K. Combined determination of highly sensitive troponin T and copeptin for early exclusion of acute myocardial infarction : first experience in an emergency department of a general hospital. Vascular Health and Risk Management. 2011;7:509–15.

33. Dittmer WU, Evers TH, Hardeman WM, Huijnen W, Kamps R, Kievit P De, et al. Rapid , high sensitivity , point-of-care test for cardiac troponin based on optomagnetic biosensor. Clinica Chimica Acta [Internet]. 2010;411(11–12):868–73. Available from: http://dx.doi.org/10.1016/j.cca.2010.03.001

34. Silva BVM, Cavalcanti IT, Mattos AB, Moura P, Del M, Sotomayor PT, et al. Disposable immunosensor for human cardiac troponin T based on streptavidin-microsphere modified screen-printed electrode. Biosensors and Bioelectronics. 2010;26:1062–7.

35. Ahammad AJS, Choi Y, Koh K, Kim J, Lee J. Electrochemical Detection of Cardiac Biomarker Troponin I at Gold Nanoparticle-Modified ITO Electrode by Using Open Circuit Potential. Int J Electrochem Sci,. 2011;6:1906–16.

36. Iskierko Z, Sharma PS, Prochowicz D, Fronc K, Souza FD, Toczydlowska D, et al. Molecularly Imprinted Polymer (MIP) Film with Improved Surface Area Developed by Using Metal- Organic Framework (MOF) for Sensitive Lipocalin (NGAL) Determination. ACS Applied Materials & Interfaces. 2016;

37. Habib S, Ghodsi E, Abdollahi S, Nadri S. Porous graphene oxide nanostructure as an

excellent scaffold for label-free electrochemical biosensor : Detection of cardiac troponin I. Materials Science & Engineering C [Internet]. 2016;69:447–52. Available from: http://dx.doi.org/10.1016/j.msec.2016.07.005

38. Silva BVM, Cavalcanti IT, Silva MMS, Dutra RF. Talanta A carbon nanotube screen-printed electrode for label-free detection of the human cardiac troponin T. Talanta [Internet]. 2013;117:431–7. Available from: http://dx.doi.org/10.1016/j.talanta.2013.08.059

39. Zavar HA, Chamsaz M, Turner APF, Tiwari A. An ultrasensitive molecularly-imprinted human cardiac troponin sensor. Biosensors and Bioelectronic [Internet]. 2013; Available from: http://dx.doi.org/10.1016/j.bios.2013.07.013

40. Dias ACMS, Silva MMS, Silva BVM, Dutra RF. A carbon nanotube-based electrochemical immunosensor for cardiac troponin T. Microchemical Journal [Internet]. 2013;109:10–5. Available from: http://dx.doi.org/10.1016/j.microc.2012.05.033

41. Pedrero M, Campuzano S, Pingarrón JM, M. Pedrero, S. Campuzano JMP. Electrochemical biosensors for the determination of cardiovascular markers: a review,. Electroanalysis. 2014;26:1132–1153.

42. Sharma V, Puri NK, Singh RK, Biradar AM, Mulchanadani A, Sharma V, et al. Label-free detection of cardiac troponin-I using gold nanoparticles functionalized single-walled carbon nanotubes based chemiresistive biosensor Label-free detection of cardiac troponin-I using gold nanoparticles functionalized single-walled carbon nanotu. Applied Physics Letters. 2013;103:203703–8.

43. Jo H, Gu H, Jeon W, Youn H, Her J, Kim S, et al. Electrochemical Aptasensor of Cardiac Troponin I for the Early Diagnosis of Acute Myocardial Infarction. Analytical Chemistry utilized. 2015;doi: 10.1021/acs.analchem.5b02312.

44. Dorraj GS, Rassaee MJ, Latifi AM, Pishgoo B, Tavallaei M. Selection of DNA aptamers against Human Cardiac Troponin I for colorimetric sensor based dot blot application. Journal of Biotechnology [Internet]. 2015;1–7. Available from: http://dx.doi.org/10.1016/j.jbiotec.2015.05.002

45. Abdolrahim M, Rabiee M, Alhosseini SN, Tahriri M, Yazdanpanah S, Tayebi L. Development of optical biosensor technologies for cardiac troponin recognition. Analytical Biochemistry [Internet]. 2015; Available from: http://dx.doi.org/10.1016/j.ab.2015.06.003

46. Fathil MFM, Arshad MK, Gopinath SCB, Hashim U, Adzhri R, Ayub RM, et al. Diagnostics on acute myocardial infarction : Cardiac troponin biomarkers. Biosensors and Bioelectronic [Internet]. 2015;70:209–20. Available from: http://dx.doi.org/10.1016/j.bios.2015.03.037

47. Shanmugam NR, Muthukumar S, Selvam AP, Prasad S. Electrochemical nanostructured ZnO biosensor for ultrasensitive detection of cardiac troponin-T. Nanomedicine. 2016;11:1345–58.

48. Nezami A, Dehghani S, Nosrati R, Eskandari N. Nanomaterial-based biosensors and immunosensors for quantitative determination of cardiac troponins. Journal of Pharmaceutical and Biomedical Analysis [Internet]. 2018;159:425–36. Available from:

https://doi.org/10.1016/j.jpba.2018.07.031

49. Justino CIL, Duarte AC, Rocha-Santos TAP. Critical overview on the application of sensors and biosensors for clinical analysis. TrAC - Trends in Analytical Chemistry [Internet]. 2016;85:36–60. Available from: http://dx.doi.org/10.1016/j.trac.2016.04.004

50. Liu D, Lu X, Yang Y, Zhai Y, Zhang J, Li L. A novel fluorescent aptasensor for the highly sensitive and selective detection of cardiac troponin I based on a graphene oxide platform. Analytical and Bioanalytical Chemistry. 2018;410:4285–91.

51. Fan Y, Jiang M, Gong D, Man C, Chen Y. Cardiac troponin for predicting all-cause mortality in patients with acute ischemic stroke : A meta-analysis. Bioscience Reports. :http://dx.doi.org/ 10.1042/BSR20171178.

52. Boeddinghaus J, Twerenbold R, Nestelberger T, Badertscher P, Wildi K, Puelacher C, et al. Clinical Validation of a Novel High-Sensitivity Cardiac Troponin I Assay for Early Diagnosis of Acute Myocardial Infarction. Clinical Chemistry. 2018;64(9):000–9.

53. Sarangadharan I, Regmi A, Chen Y, Hsu C, Chen P, Chang H, et al. High sensitivity cardiac troponin I detection in physiological environment using AlGaN / GaN High Electron Mobility Transistor (HEMT) Biosensors. Biosensors and Bioelectronic [Internet]. 2018;100:282–9. Available from: http://dx.doi.org/10.1016/j.bios.2017.09.018

54. Qiao X, Li K, Xu J, Cheng N, Sheng Q, Cao W, et al. Novel electrochemical sensing platform for ultrasensitive detection of cardiac troponin I based on aptamer-MoS 2 nanoconjugates. Biosensors and Bioelectronic [Internet]. 2018;113:142–7. Available from: https://doi.org/10.1016/j.bios.2018.05.003

55. Upasham S, Tanak A, Prasad S. Cardiac troponin biosensors : where are we now ? Advanced Health Care Technologies. 2018;4:1–13.

56. Han X, Kojori HS, Leblanc RM, Kim SJ. Ultrasensitive Plasmonic Biosensors for Real-Time Parallel Detection of Alpha-L-Fucosidase and Cardiac-Troponin-I in Whole Human Blood Ultrasensitive Plasmonic Biosensors for Real-Time Parallel Detection of Alpha-L-Fucosidase and Cardiac-Troponin-I in Who. Anal Chem. 2018;DOI: 10.1021/acs.analchem.8b01816.

57. Hickman PE, Koerbin G, Badrick T, Oakman C, Potter JM. The importance of low level QC for high sensitivity troponin assays. Clinical Biochemistry [Internet]. 2018;(April):0–1. Available from: https://doi.org/10.1016/j.clinbiochem.2018.05.007

58. Zhou W, Li K, Wei Y, Hao P, Chi M, Liu Y. Ultrasensitive label-free optical micro fi ber coupler biosensor for detection of cardiac troponin I based on interference turning point e ff ect. Biosens Bioelectron [Internet]. 2018;106(October 2017):99–104. Available from: https://doi.org/10.1016/j.bios.2018.01.061

59. Chen J, Kong L, Sun X, Feng J, Chen Z, Fan D, et al. Ultrasensitive photoelectrochemical immunosensor of cardiac troponin I detection based on dual inhibition effect of Ag@Cu2O core-shell submicron-particles on CdS QDs sensitized TiO2 nanosheets. Biosens Bioelectron [Internet]. 2018; Available from: https://doi.org/10.1016/j.bios.2018.05.037

60. Kavsak PA. US CR. Clinical Biochemistry [Internet]. 2018;#pagerange#. Available from:

https://doi.org/10.1016/j.clinbiochem.2018.05.015

61. Yan H, Tang X, Zhu X, Zeng Y, Lu X, Yin Z, et al. Sandwich-type electrochemical immunosensor for highly sensitive determination of cardiac troponin I using carboxyl-terminated ionic liquid and helical carbon nanotube composite as platform and ferrocenecarboxylic acid as signal label. Sensors & Actuators: B Chemical [Internet]. 2018; Available from: https://doi.org/10.1016/j.snb.2018.09.010

62. Beausire T, Faouzi M, Palmiere C, Fracasso T, Michaud K. High-sensitive cardiac troponin hs-TnT levels in sudden deaths related to atherosclerotic coronary artery disease. Forensic Science International [Internet]. 2018; Available from: https://doi.org/10.1016/j.forsciint.2018.05.051

Appendix B:

2.1. Materials

All solvents and chemicals used in this study were of analytical reagent grade and were used as received. Polyvinyl chloride powder PVC of high molecular weight, o-nitrophenyl octyl ether (o-NPOE), dioctyl phthalate (DOP), dioctyl sebacate (DOS), tetrahydrofuran (THF) of purity greater than 99 %, 1, 2-phenylenediamine $C_6H_8N_2$; melting point 100-102 °C; 99.5%; and $MnCl_2.4H_2O$; 99.99% were purchased from Sigma-Aldrich. 5-aminoisophthalic acid $C_8H_7NO_4$; melting point greater than 300 °C; 98%; was purchased from Acros-organics. Standard cardiac troponin (cTn) protein of different buffered concentrations were supplied by Monobind, USA.

2.2. Instruments

The characterization and applications were performed using different analytical techniques: The mass spectra of solid NL and Mn-MOF were recorded using a Thermo Scientific- ISQ single quadrupole mass spectrometer. The ^{1}H-NMR and ^{13}C-NMR spectra of samples in deuterated dimethylsulfoxide (DMSO-D^{6}) were performed with a 500 MHz NMR spectrometer (JEOL-ECA 500II). Elemental analysis (C-H-N) were performed using a Costech ECS-4010- analyzer. The Fourier transform-infrared (FT-IR) spectra were recorded with a JASCO FT/IR-460 spectrophotometer with use of KBr tablets in the range from 400 to 4000 cm^{-1} at room temperature. The UV-vis spectra for samples by were obtained using V-770 UV-Visible/NIR spectrophotometer over a range from 200 to 2200 nm, and the band gap calculated with Optbandgap-204B soft wear. X-ray diffraction (XRD) of Mn-MOF was performed with a D8-AVANCE X-ray diffractometer (Bruker AXS, Germany) with Cu-Kα radiation (λ =0.154056 nm) for identification of the crystalline phase, relative crystallinity and crystal size of as-prepared Mn-MOF. The sample was identified in the 2θ range from 3.105° to 70.086° with a 0.020° step at a scan speed of 0.4 s. The crystallite size was calculated from XRD data by means of the Scherer equation. The oxidation states and species in the prepared materials were recorded by Thermo Scientific™ K-Alpha™ XPS spectrometer, Al-Kα micro-focused monochromator within an energy range up to 4 KeV. The FE-SEM images and EDX spectroscopy spectra were recorded with a combination of field emission scanning electron microscopy (FE-SEM), and element mapping by spatially resolved energy-dispersive X-ray spectroscopy (EDX)

(JEOL JSM-6510LV advanced electron microscope with a LAB-6 cathode at 520 keV). The structures of the phases formed were examined by using a high-resolution transmission electron microscope (HR-TEM) with an acceleration voltage up to 200 kV (JEM-2100-JEOL, Japan). Thermal analysis (DSC/TGA) of the samples were analyzed with a NETZSCH STA 409 C/CD, Germany with a rate of 10 °C min^{-1} in nitrogen atmosphere. The magnetic properties of the fabricated sample was accomplished using a vibrating sample magnetometer (7400-1 VSM, U.S., Lake Shore Co., Ltd., USA) in a maximum applied field of 20 kOe. The photoluminescence (PL) spectra were investigated using a (Shimadzu RF-5301PC spectrofluorophotometer). The samples were used for subsequent PL measurements at different excitation wavelengths and then at an excitation wavelength 300 nm and an emission wavelength of 422 nm. The measurements were performed in a quartz cuvette of path length 1 cm, with a scan time of 30 s, at room temperature. All potentiometric measurements were performed at room temperature with constant magnetic stirring, with an Orion Model A720 digital pH/mV meter and an Orion Ross Combination pH electrode (Model 81-02) for all pH measurements. Mn-MOF-PVC based electrode was used for all potentiometric measurements in conjunction with a double junction reference electrode (Orion Model 90-02) containing KNO_3 (10% w/v) in the outer compartment\silver-silver chloride reference electrode. The data were analyzed with Origin-8. The structures, 3D geometrical structures and Schemes were drawn using "ChemBioDraw Ultra12" program.

Appendix C:

Design of the device

The suggested device can be able to connect to the potentiometric electrode sensor through a calibration program. The sensor will be able to detect any changing in the potential response and send an information to the device. The device will receive the data from the sensor and will be analyze it. The smart program which prepared in an internal memory using calibrated data will be appeared on LCD screen. The new device will consist from the microcontroller board, PIC 16F887 IC, battery, keypad, project box and sensors. A small device controlled with one hand (POCT device) in the end will be fabricated, with a size approximately 15 cm length, width 10 cm and height 4 cm.